

# Wave dispersion under finite deformation

Mohammad H. Abedinnasab<sup>a</sup>, Mahmoud I. Hussein<sup>b,\*</sup>

<sup>a</sup>*Department of Mechanical Engineering, Sharif University of Technology, Tehran,  
11365-9567, Iran*

<sup>b</sup>*Department of Aerospace Engineering Sciences, University of Colorado Boulder,  
Boulder, CO 80309-0429, USA*

---

## Abstract

We derive exact dispersion relations for axial and flexural elastic wave motion in a rod and a beam under finite deformation. For axial motion we consider a slender rod model, and for flexural motion we employ the Euler-Bernoulli kinematic hypothesis and consider both a conventional transverse motion model and an inextensional planar motion model. The underlying formulation uses the Cauchy stress and the Green-Lagrange strain without omission of higher order terms. For all models, we consider linear constitutive relations in order to isolate the effect of finite motion. The proposed methodology, however, is applicable to problems that also exhibit material nonlinearity. For the rod model, we obtain the exact analytical explicit solution of the derived finite-deformation dispersion relation, and compare it with data obtained via numerical simulation of nonlinear wave propagation in a finite rod. For the beam model, we obtain an approximate solution by standard root finding. The results allow us to quantify the deviation in the dispersion curves when exact large deformation is considered compared to following the assumption of infinitesimal deformation. We show that incorporation of finite deformation following the chosen definitions of stress and strain raises the frequency branches for both axial and flexural waves and consequently also raises the phase and group velocities above the nominal values associated with linear motion. For the beam problem, only the inextensional planar motion model provides an accurate description of the finite-deformation response for both static deflection and wave dispersion; the conventional transverse motion model fails to do so. Our findings, which represent the first derivation of finite-strain dispersion relations for any type of elastic media, draw attention to (1) the tangible effect of finite deformation on wave dispersion and consequently on the speed of sound in an elastic

medium and (2) the importance of incorporating axial-transverse motion coupling in both static and dynamic analysis of thin structures subjected to large nonlinear deformation.

---

## 1. Introduction

The dispersion relation provides a fundamental characterization of the nature of wave propagation in an elastic solid. Its derivation for various solid configurations, such as beams, plates, surfaces etc., has been key to the development of the field of elastic wave propagation, a field that traces its beginnings to the seminal memoir of Poisson [1]. In this memoir, and in the work of Cauchy [2], it was revealed that two types of waves exist in solids: longitudinal and transverse. Analysis of the dispersive nature of these waves in different types of unbounded structures has been a focus of many classical studies since then. Brief surveys on the historical development of theoretical elastic wave propagation research are provided by Graff [3] and Ben-Menahem [4], and a thorough discussion on the reconciliation of theory with experiments on mechanical waves is given by Thurston [5].

These early investigations as well as the vast majority of contemporary studies of wave propagation in elastic solids are based primarily on linear analysis, that is, linear constitutive laws and linear strain-displacement relationships are assumed (see [3], [6], and references therein). The incorporation of nonlinear effects has nevertheless been actively pursued and continues to attract attention as it allows for a more accurate description of the underlying motion and facilitates the study of amplitude-dependent wave interaction phenomena that do not appear in linear systems (see the monograph on nonlinear oscillations by Nayfeh and Mook [7] and a recent special journal issue edited by Destrade and Saccomandi [8] for broad listings of references on the subject). From an engineering perspective, the effects of nonlinearity on the dispersion of waves in waveguides could be utilized to enrich the design of materials and structural components. In general, the study of nonlinear elastic wave propagation is relevant to nonlinear vibration analysis [9, 10], dislocation and crack dynamics analysis [11, 12], geophysical and seismic mo-

---

\*Corresponding author. Tel.: +1 303-492-3177

*Email address:* mih@colorado.edu (Mahmoud I. Hussein)

tion analysis [13, 14], material characterization and nondestructive evaluation [15, 16], biomedical imaging [17], and others.

Finite amplitude wave propagation in elastic solids is a subset among the broader class of nonlinear wave propagation problems. From a mathematical perspective, a formal treatment of finite deformation requires the incorporation of an exact nonlinear strain tensor in setting up the governing equations of motion. As a result, the emerging analysis should permit large and finite strain fields, as opposed to small and infinitesimal strain fields. A large portion of research on finite amplitude waves considers initially strained materials (see, for example, the early studies by Truesdell [18] and Green [19], and Ogden [20] for an extensive discussion on the topic). Among the relatively recent works that focused on finite-amplitude plane waves in materials subjected to a large static finite deformation include those of Boulanger and Hayes [21], Boulanger et al. [22] and Destrade and Saccomandi [23]. Furthermore, analysis of finite-amplitude waves in solids often involve small parameters or asymptotic expansions (see Norris [24] for a review). Auld [25], for example, and subsequent studies by de Lima and Hamilton [26], Deng [27] and Srivastava et al. [28], treated the problem of finite-strain waves using normal mode expansion and forced response calculations. This approach is based on perturbation theory and is therefore limited to small amplitudes. Focusing on rods, modeled in one dimension or higher, many studies considered finite amplitude waves for both incompressible and compressible materials (e.g., [5, 29–33]). Of particular relevance is a recent investigation by Zhang and Liu [34] in which an exact equation of motion for a rod and an approximate equation of motion for an Euler-Bernoulli beam were derived under the condition of finite deformation. It is rather common in the study of structural waveguides to omit (for simplicity) some terms in the strain tensor at the outset, and among the strain tensor terms that are retained some emerging high order terms associated with the deformation of the cross-sectional frame are often neglected.

A broad overview of the listed references and other finite-deformation-based studies in the literature reveals that generally the interest has been in obtaining spatial/temporal solutions, or solutions at certain physical limits, rather than complete dispersion relations that directly relate frequency to wavevectors (or wavenumbers). In this paper, we provide an exact analysis of static deflection and elastic wave dispersion in a rod and a beam under finite deformation with no modeling limitation on the amplitude of the deflection or the travelling wave. Starting with Hamilton’s principle we consider both

axial deformation (to represent longitudinal motion in a rod) and flexural deformation (to represent transverse or axial-transverse motion in a beam). Focusing on homogeneous waveguides with constant cross-section and non-dissipative, isotropic material properties, we derive the exact equation of motion and dispersion relation.<sup>1</sup> For the rod problem, we subsequently obtain the explicit frequency versus wavenumber solution. For the flexural beam problem, we obtain a solution by numerically finding the roots of the derived dispersion relation. In all our derivations, we use the Cauchy and Green-Lagrange definitions of stress and strain, respectively. Furthermore, all terms in the nonlinear strain tensor are retained and no high order terms emerging from the differentiation are subsequently neglected. In order to isolate the effect of finite motion, we consider linear constitutive relations. The proposed methodology, however, is applicable to problems that also exhibit material nonlinearity. To validate our theoretical approach, we first consider static deflection, in both a rod and a beam, and make comparisons with finite element (FE) solutions based on exact elasticity theory. We then consider the dynamics regime, where for the rod problem we examine wave propagation in a finite rod by means of standard finite-strain numerical simulations (also using FE analysis) and compare the full-spectrum response with our derived dispersion relation.

The dispersion formulations we develop in this work, which represent the first derivation of finite-strain dispersion relations for any type of elastic media, allow us to examine (1) the effect of finite deformation on the frequency and phase/group velocity dispersion curves in rods and beams and (2) the role that axial-transverse motion coupling plays in the underlying nonlinear mechanics of flexural beams.

## 2. Rod and beam kinematics based on finite deformation

### 2.1. Classification of rod and beam kinematics

In this paper we study geometrically nonlinear wave propagation in a rod and in a flexural beam, assuming slender structure for each case. To put the kinematical description of the problems we consider in context, we show in Table 1 the categories of the various possible approximate theories for

---

<sup>1</sup>A derivation of finite-strain dispersion for a beam model based on an approximate equation of motion was published earlier by the authors [35]

the treatment of a rod/beam, ranging from 1 to 4 degree-of-freedom (DOF) systems. The table lists axial motion for a rod (one model), planar motion for a beam (three models) and spatial motion for a beam (two models). Each model is described fundamentally by the number and type of variables, the form of the exact displacement field,  $\Delta$ , and the constraint (if any) that applies to the displacement field variables.

The rod model admits axial motion, tension or compression, with  $u$  denoting its axial displacements. In the conventional beam model, the axial displacements are assumed to be zero. Hence, the only variable is  $v$ , which denotes the lateral displacements. The planar beam models admit both  $u$  and  $v$  displacements and provide a coupling relationship between these two variables. Figure 1 provides graphical descriptions of the kinematics of a planar beam showing the variables in the  $s - y$  plane, where  $s$  is the Lagrangian longitudinal coordinate. The third axis perpendicular to  $s$  and  $y$  is denoted by  $z$ . In a general planar beam model, the following kinematic relationship holds:  $e = r - 1$ , where  $e$  is the axial strain of the centerline and  $r = \sqrt{(1 + u')^2 + v'^2}$ . The inextensional planar beam model is a special case of the general planar beam model, in which an inextensionality constraint is applied such that the axial strain of the beam's centerline is assumed to be zero. This provides us with the following relationship:

$$u' = \sqrt{1 - v'^2} - 1. \quad (1)$$

Application of an inextensionality constraint to a beam with any type of boundary conditions is known to be generally adequate in the absence of large axial forces (Drespo da Silva and Glynn [36]; Nayfeh and Pai [37]; Lacarbonara and Yabuno [38]). In all planar beam models, it is assumed that the cross-section remains plane and perpendicular to the centerline after elastic deformation. In addition, it is assumed that in-plane and out-of-plane warpings of the cross-section do not occur. These assumptions are justified, even for large finite deformation, in light of our focus on beams with aspect ratios high enough for the Euler-Bernoulli kinematic hypothesis to be valid. In the spatial beam models, the beam admits four degrees of freedom,  $u$ ,  $v$ ,  $w$ , and  $\gamma$ , where  $w$  denotes the lateral displacements in a direction perpendicular to  $u$  and  $v$ , and  $\gamma$  is the torsion angle of the cross-section. Here the displacement field is written in terms of the matrix  $R_{BS}$ ,

which is defined as

$$R_{BS} = \begin{bmatrix} \cos \alpha & -\sin \alpha & 0 \\ \sin \alpha & \cos \alpha & 0 \\ 0 & 0 & 1 \end{bmatrix} \begin{bmatrix} \cos \beta & 0 & \sin \beta \\ 0 & 1 & 0 \\ -\sin \beta & 0 & \cos \beta \end{bmatrix} \begin{bmatrix} 1 & 0 & 0 \\ 0 & \cos \gamma & -\sin \gamma \\ 0 & \sin \gamma & \cos \gamma \end{bmatrix}$$

in which  $\alpha = \arctan v'/h$  and  $\beta = -\arctan w'/r$ , where  $h$  is an agent variable defined as

$$h = 1 + u', \quad (2)$$

and  $r = \sqrt{h^2 + v'^2}$ . We note that  $\alpha$  and  $\beta$  are dependent variables representing the in-plane and out-of-plane deflection angles, where the torsion angle  $\gamma$  is an independent variable. In a similar manner to the planar models, an inextensionality constraint can be applied to produce the inextensional spatial beam model. The advantage of the inextensionality constraint is that it reduces the number of DOF of a system by one, as indicated in Table 1. The cases we consider in this work (rod, conventional beam and inextensional planar beam) are all 1 DOF systems. Future work will address finite-strain wave dispersion behavior of higher DOF systems (see [39] for a static treatment of higher DOF systems).

## 2.2. Finite strain fields of single DOF models

In Section 3, we derive the equation of motion for our three models on the basis of the Green-Lagrange strain tensor. In the following subsections, the form of the Green-Lagrange strain tensor is given, for a rod and for a beam. Other measures of strain may be chosen. However, in this work, we only use the Green-Lagrange strain owing to its wide use in the literature.

### 2.2.1. Rod: Finite strain field

Introducing  $\Delta$  to generally represent elastic displacement, the Green-Lagrange strain field in a rod is given by

$$\epsilon = \frac{\partial \Delta}{\partial s} + \frac{1}{2} \left( \frac{\partial \Delta}{\partial s} \right)^2, \quad (3)$$

where the first and second terms on the RHS represent the linear and non-linear parts, respectively. As seen in Table 1, the elastic displacement field,  $\Delta$ , is scalar for a rod and is equal to the axial displacement,  $u$ .

Table 1: Rod and beam kinematic models

Description	Motion/DOF	Indep. Variable(s)	Displacement field, $\Delta$	Constraint
Rod	Axial/1	$u$	$u$	—
Conventional beam	Transverse/1	$v$	$\begin{bmatrix} -yv'/\sqrt{1+v'^2} \\ v - y(1 - 1/\sqrt{1+v'^2}) \end{bmatrix}$	—
Inextensional planar beam	Planar/1	$u, v$	$\begin{bmatrix} u - yv'/r \\ v - y(r - h)/r \end{bmatrix}$	$r - 1 = 0$
Planar beam	Planar/2	$u, v$	$\begin{bmatrix} u - yv'/r \\ v - y(r - h)/r \end{bmatrix}$	—
Inextensional spatial beam	Spatial/3	$u, v, w, \gamma$	$\begin{bmatrix} u \\ v \\ w \end{bmatrix} + (R_{BS} - I) \begin{bmatrix} 0 \\ y \\ z \end{bmatrix}$	$\sqrt{r^2 + w'^2} - 1 = 0$
Spatial beam	Spatial/4	$u, v, w, \gamma$	$\begin{bmatrix} u \\ v \\ w \end{bmatrix} + (R_{BS} - I) \begin{bmatrix} 0 \\ y \\ z \end{bmatrix}$	—

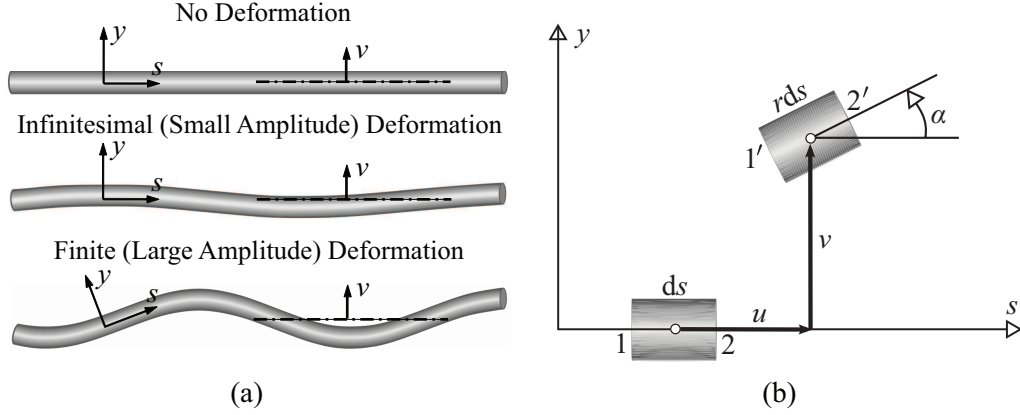


Figure 1: Kinematical representation of a planar flexural beam model: (a) infinitesimal versus finite deformation, (b) illustration of the variables  $u$  and  $v$  and the rotation angle  $\alpha$ , noting that  $r = 1 + e$  where  $e$  is the strain of the centerline.

### 2.2.2. Beam: Finite strain field

In analogy to (3), the Green-Lagrange strain tensor for a beam is

$$\epsilon_{ij} = \frac{1}{2} \left( \frac{\partial \Delta_i}{\partial x_j} + \frac{\partial \Delta_j}{\partial x_i} + \frac{\partial \Delta_m}{\partial x_i} \frac{\partial \Delta_m}{\partial x_j} \right), \quad (4)$$

where  $i$  and  $j$  take the value of 1 or 2, in which  $x_1 = s$  and  $x_2 = y$  (see Fig. 1 and Table 1). For conventional and inextensional beams,  $\Delta$  represents the elastic displacement vector, which is  $[-yv'/\sqrt{1+v'^2} \quad v - y(1 - 1/\sqrt{1+v'^2})]^T$  and  $[u - yv'/r \quad v - y(r - h)/r]^T$ , respectively.

### 3. Equations of motion based on finite deformation

In this section we derive the equation of motion for a rod (Section 3.1), a conventional beam (Section 3.2) and an inextensional planar beam (Section 3.3). In our derivations, we consider non-dissipative, isotropic media and assume constant material and geometric properties. Furthermore, we ignore the effect of lateral inertia on the axial motion.

#### 3.1. Rod: Axial motion

Using Hamilton's principle, we write the equation of motion for a rod under uniaxial stress as

$$\int_0^t (\delta T - \delta U^e + \delta W^{nc}) dt = 0, \quad (5)$$

where  $T$ ,  $U^e$ , and  $W^{nc}$  denote kinetic energy, elastic potential energy and work done by external non-conservative forces and moments, respectively, and  $t$  denotes time. Using integration by parts, the variation of kinetic energy is

$$\delta T = -\rho A \int_0^l (\ddot{u} \delta u) ds. \quad (6)$$

where  $l$  denotes the length of an arbitrary portion of the rod, and  $\rho$  and  $A$  denote density and cross-sectional area, respectively. The variation of elastic potential energy is also obtained using integration by parts and is given as

$$\delta U^e = \int_0^l \int_A (\sigma \delta \epsilon) dA ds, \quad (7)$$

where  $\sigma$  and  $\epsilon$  are the axial stress and axial strain, respectively. In this work we base our analysis on the Cauchy stress and consider a linear stress-strain relationship as given by Hooke's law, that is,  $\sigma = E\epsilon$ , where  $E$  is the Young's



modulus. Using Eq. (7), and with the aid of integration by parts, we can now write the variation of elastic potential energy as

$$\delta U^e = \int_0^l \left\{ \frac{1}{2} E A h (h^2 - 1) \delta u' \right\} ds, \quad (8)$$

where  $u' = du/ds = u_s$  and  $h$  is as defined in Eq. (2). The variation of the work done by non-conservative forces and moments is given in terms of the variation of axial deformation,  $u$ , and the distributed external axial load,  $q_u$ ,

$$\delta W^{nc} = \int_0^l (q_u \delta u) ds. \quad (9)$$

Substitution of Eqs. (6), (8) and (9) into Eq. (5) produces the equation of motion (10) and the companion boundary conditions (11):

$$\int_0^t \left\{ \int_0^l (A_1 \delta u) ds + (B_1 \delta u + \overline{B_1} \delta u') \Big|_{s=0}^{s=l} \right\} dt = 0, \quad (10)$$

$$(B_1 = 0 \quad \text{or} \quad u = 0) \quad \text{and} \quad (\overline{B_1} = 0 \quad \text{or} \quad u' = 0). \quad (11)$$

We can now write an exact nonlinear equation of motion of a one-dimensional (1D) rod under finite deformation as

$$A_1 = 0 : \quad \rho A \ddot{u} = \frac{1}{2} E A (3h^2 - 1) u'' + q_u. \quad (12)$$

The section loads are

$$B_1 = \frac{1}{2} E A h (h^2 - 1) \quad \text{and} \quad \overline{B_1} = 0, \quad (13)$$

where  $B_1$  is the axial force. If the axial deformation is infinitesimal, then  $u'$  is small and from Eq. (2),  $h \approx 1$ . Substitution of  $h = 1$  into Eq. (12) leads to

$$A_1 = 0 : \quad \rho A \ddot{u} = E A u'' + q_u. \quad (14)$$

which is the equation of motion describing infinitesimal axial deformation.

### 3.2. Conventional beam: Transverse motion

Using Hamilton's principle, we state the equation of motion as follows:

$$\int_0^t (\delta T - \delta U^g - \delta U^e + \delta W_{nc}) dt = 0. \quad (15)$$

We express the elastic deformation using the flexural displacement  $v$  as well as the angular displacement  $\alpha$ . These two elastic coordinates are related by the following holonomic constraint:  $\alpha = \tan^{-1}(dv/ds) = \tan^{-1}v'$ . The variation of kinetic energy, with the aid of integration by parts, is

$$\begin{aligned} \delta T = & -\rho \int_0^l \left\{ A\ddot{v} - \left( \frac{1}{r^2} J\ddot{\alpha} \right)' \right\} \delta v ds \\ & - \rho \left\{ \left( \frac{1}{r^2} J\ddot{\alpha} \right) \delta v \right\} \bigg|_{s=0}^{s=l}, \end{aligned} \quad (16)$$

where  $J$  is the second moment of cross-sectional area, defined as

$$J = \int_A y^2 dA = \int_A z^2 dA = \frac{\pi}{4} a^4. \quad (17)$$

In Eq. (16),  $r$  is defined as  $r = \sqrt{1 + v'^2}$ . The variation of gravitational potential energy is

$$\delta U^g = g\rho A \int_0^l (\delta v) ds. \quad (18)$$

where  $g$  denotes acceleration due to gravity. As in the rod case, we use the Cauchy stress and the standard linear Hooke's law in our formulation. Since we are not permitting in-plane and out-of-plane warpings of the cross-section, we set the Poisson's ratio,  $\nu$ , to zero in the constitutive relationship. The variation of elastic potential energy can now be written as

$$\delta U^e = \int_0^l \int_A (\sigma_{ss} \delta \epsilon_{ss} + \sigma_{yy} \delta \epsilon_{yy} + 2\sigma_{sy} \delta \epsilon_{sy}) dA ds. \quad (19)$$

After substituting Eq. (4) and the constitutive relationship into (19), we obtain

$$\delta U^e = \int_0^l \{C_{vp}\delta v' + C_{vpp}\delta v''\}ds. \quad (20)$$

where the coefficient of  $\delta v'$  is

$$C_{vp} = \frac{1}{2}EA(v')^3 + \frac{EJ(2 - 3r^2)v'(v'')^2}{2r^6} - \frac{EJ_f v'(v'')^4}{r^{10}}, \quad (21)$$

and the coefficient of  $\delta v''$  is

$$C_{vpp} = \frac{EJ_f(v'')^3}{2r^8} - \frac{EJ(1 - 3r^2)v''}{2r^4}. \quad (22)$$

In Eqs. (21) and (22),  $J_f$  is the 4<sup>th</sup> moment of cross-sectional area, defined as

$$J_f = \int_A y^4 dA = \int_A z^4 dA = \frac{\pi}{8}a^6. \quad (23)$$

It is also useful to define  $J_c$ , the higher-order product of cross-sectional area,

$$J_c = \int_A y^2 z^2 dA = \frac{\pi}{24}a^6. \quad (24)$$

Both  $J_f$  and  $J_c$  have been calculated for a circular cross-section with radius  $a$ . It can be seen from Eqs. (23) and (24) that for a circular cross-section beam,  $J_f = 3J_c$ . The variation of the work done by non-conservative forces and moments is given in terms of the variation of the flexural displacement and the distributed external load,

$$\delta W_{nc} = \int_0^l (q_v \delta v) ds. \quad (25)$$

Substitution of Eqs. (16), (18), (20) and (25) into Eq. (15) generates the equation of motion (26) and the companion boundary conditions (27),

$$\int_0^t \left\{ \int_0^L (A_2 \delta v) ds + (B_2 \delta v + \overline{B_2} \delta v') \Big|_{s=0}^{s=L} \right\} dt = 0, \quad (26)$$

$$(B_2 = 0 \quad \text{or} \quad v = 0) \quad \text{and} \quad (\overline{B_2} = 0 \quad \text{or} \quad v' = 0). \quad (27)$$

Consequently, an exact nonlinear equation of motion for a conventional Euler-Bernoulli beam based on finite deformation is

$$A_2 = 0 : \quad -\rho Ag - \rho A\ddot{v} + \rho J \left( \frac{\ddot{\alpha}}{r^2} \right)' + q_v + (C_{vp})' - (C_{vpp})'' = 0. \quad (28)$$

After substituting the  $C_{vp}$  and  $C_{vpp}$  coefficients from Eqs. (21) and (22) and simplifying, we obtain the closed-form equation of motion for a conventional beam,

$$\begin{aligned} A_2 = 0 : & -\rho Ag - \rho A\ddot{v} + \rho J (\ddot{\alpha})' + q_3 + \frac{3EA(v')^2 v''}{2} + \frac{2EJv'(1+3(v')^2)v''v^{(3)}}{(1+(v')^2)^3} \\ & - \frac{EJ(2+3(v')^2)v^{(4)}}{2(1+(v')^2)^2} + \frac{EJ(1+4(v')^2-9(v')^4)(v'')^3}{2(1+(v')^2)^4} - \frac{3EJ_f(v'')^2v^{(4)}}{2(1+(v')^2)^4} \\ & + \frac{24EJ_f v'(v'')^3 v^{(3)}}{(1+(v')^2)^5} + \frac{3EJ_f(1-9(v')^2)(v'')^5}{(1+(v')^2)^6} - \frac{3EJ_f v''(v^{(3)})^2}{(1+(v')^2)^4} = 0. \end{aligned} \quad (29)$$

The section loads, namely the transverse shear force and the bending moment, are respectively

$$B_2 = \rho J \left( \frac{\ddot{\alpha}}{r^2} \right) + C_{vp} - (C_{vpp})' \quad \text{and} \quad \overline{B}_2 = C_{vpp}. \quad (30)$$

### 3.3. Inextensional planar beam: Axial-transverse motion

Following Hamilton's principle, the inextensionality constraint as stated in Eq. (1), and its corresponding Lagrange multiplier,  $\vartheta$ , we write

$$\int_0^t (\delta T - \delta U^g - \delta U^e + \delta W_{nc} + \delta(\vartheta \cdot e)) dt = 0. \quad (31)$$

Accounting for rotary inertia, we write the total kinetic energy of the beam as

$$T = 1/2\rho \int_0^L \{A(\dot{u}^2 + \dot{v}^2) + J\dot{\alpha}^2\} ds. \quad (32)$$

The variation of kinetic energy is then obtained with the aid of integration by parts,

$$\begin{aligned} \delta T = & -\rho \int_0^L \left\{ \left\{ A \begin{bmatrix} \ddot{u} & \ddot{v} \end{bmatrix} - \begin{bmatrix} -\frac{v'}{r^2} J \ddot{\alpha} & \frac{h}{r^2} J \ddot{\alpha} \end{bmatrix}' \right\} \begin{bmatrix} \delta u \\ \delta v \end{bmatrix} \right\} ds \\ & - \rho \left[ \begin{bmatrix} -\frac{v'}{r^2} J \ddot{\alpha} & \frac{h}{r^2} J \ddot{\alpha} \end{bmatrix} \begin{bmatrix} \delta u \\ \delta v \end{bmatrix} \right] \bigg|_{s=0}^{s=l}, \end{aligned} \quad (33)$$

Substituting Eq. (4) and the linear constitutive relationship into Eq. (19) yields the unknown coefficients of the variation of elastic potential energy in Eq. (20). The coefficient of  $\delta v'$  in Eq. (20) is

$$C_{vp} = - \left( J + \frac{J_f(1 + 2v'^2)v''^2}{2(1 - v'^2)} \right) \frac{Ev'v''^2}{(1 - v'^2)^2} - \left( J + \frac{3v''^2}{2(1 - v'^2)} \right) \frac{Ev'^2v^{(3)}}{1 - v'^2}. \quad (34)$$

Similarly, the coefficient of  $\delta v''$  in Eq. (20) is

$$C_{vpp} = \left( J + \frac{J_f v''^2}{2(1 - v'^2)} \right) Ev''. \quad (35)$$

Substitution of Eqs. (33), (18), (20) and (25) into Eq. (31) generates the equation of motion (36) and the companion boundary conditions (37),

$$\int_0^t \left\{ \int_0^L (A_2 \delta v) ds + (B_2 \delta v + \overline{B}_2 \delta v') \bigg|_{s=0}^{s=L} \right\} dt = 0, \quad (36)$$

$$(B_2 = 0 \quad \text{or} \quad v = 0) \quad \text{and} \quad (\overline{B}_2 = 0 \quad \text{or} \quad v' = 0). \quad (37)$$

Consequently, an exact nonlinear equation of motion for an inextensional Euler-Bernoulli beam based on finite deformation is

$$A_2 = 0 : \quad -\rho Ag - \rho A \ddot{v} + \rho J \left( \frac{\ddot{\alpha}}{r^2} \right)' + q_v + (C_{vp})' - (C_{vpp})'' = 0. \quad (38)$$

After substituting the  $C_{vp}$  and  $C_{vpp}$  coefficients from Eqs. (34) and (35) and simplifying, we obtain the closed-form equation of motion for an inextensional planar beam,

$$\begin{aligned}
A_2 = 0 : & -\rho Ag - \rho A\ddot{v} + \rho J \left( \frac{\ddot{\alpha}}{h} \right)' - \left[ \frac{v'}{\sqrt{1-v'^2}} \left( \int_x^l (\rho A\ddot{u} - q_2) ds \right) \right]' + q_3 \\
& - \frac{EJv^{(4)}}{1-(v')^2} - \frac{4EJv'v''v^{(3)}}{(1-(v')^2)^2} - \frac{EJ(1+3(v')^2)(v'')^3}{(1-(v')^2)^3} - \frac{3EJ_f(v'')^2v^{(4)}}{2(1-(v')^2)^2} \\
& - \frac{12EJ_fv'(v'')^3v^{(3)}}{(1-(v')^2)^3} - \frac{3EJ_f(1+5(v')^2)(v'')^5}{2(1-(v')^2)^4} - \frac{3EJ_fv''(v^{(3)})^2}{(1-(v')^2)^2} = 0.
\end{aligned} \tag{39}$$

The transverse shear force and bending moment section loads are found from Eqs. (40a) and (40b), respectively.

$$\begin{aligned}
B_2 = \rho J \left( \frac{\ddot{\alpha}}{h} \right) & - \left[ \frac{v'}{\sqrt{1-v'^2}} \left( \int_x^l (\rho A\ddot{u} - q_2) ds \right) \right] \\
& - \frac{EJv'(v'')^2}{(1-(v')^2)^2} - \frac{EJv^{(3)}}{1-(v')^2} - \frac{3EJ_f(v'')^2v^{(3)}}{2(1-(v')^2)} - \frac{3EJ_fv'(v'')^4}{2(1-(v')^2)^3},
\end{aligned} \tag{40a}$$

$$\overline{B}_2 = EJv'' + \frac{EJ_f(v'')^3}{2(1-(v')^2)}. \tag{40b}$$

It is noticeable from Eqs. (23) and (17), that  $J_f$  is quantitatively small compared to  $J$  when the beam is slender (i.e., when  $a$  is small). As a result, we can neglect the terms containing  $J_f$  in Eqs. (39), (40a) and (40b) (further discussion on this omission is provided in Section 6.3). If these terms are dropped from Eq. (39) only three elastic terms remain, namely  $-\frac{EJv^{(4)}}{1-(v')^2}$ ,  $-\frac{4EJv'v''v^{(3)}}{(1-(v')^2)^2}$  and  $-\frac{EJ(1+3(v')^2)(v'')^3}{(1-(v')^2)^3}$ . The resulting equation of motion is relatively simple yet still adequate for large elastic deformation.

#### 4. Static deflection under finite deformation

In this section we consider the static deflection problem and hence omit all the inertial terms in the rod and beam equations of motion (Eqs. (12), (28)

and (39)). Figure 2 presents the static response of a rod due to the application of a force load,  $q_u$  (Section 3.1 ). We show the response following our finite-deformation formulation and that obtained using the COMSOL Multiphysics software package [40] which is based on a three-dimensional (3D) nonlinear FE model of a rod following the theory of elasticity.<sup>2</sup> The results are in excellent agreement and thus provide a validation to our rod formulation for static response. Figure 2 also shows that omission of the Poisson’ ratio has a negligible effect on the nonlinear static response. The deflection under the infinitesimal strain assumption is included for comparison.

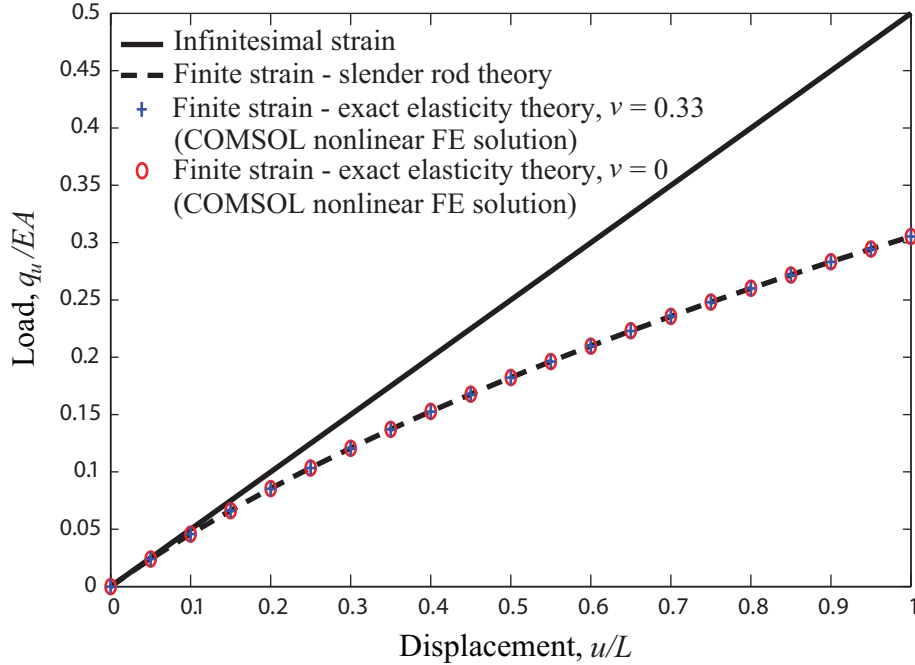


Figure 2: Static deflection of a rod.

In Fig. 3 we consider a clamped-free beam, with a length of  $L$ , under a uniform external load,  $q_v$ . In the figure we show the results obtained by our finite-deformation formulations (following the conventional transverse motion model and the inextensional planar motion model) and the result

<sup>2</sup>The COMSOL model used is “solid mechanics with geometric nonlinearity”. A fine mesh density (12,000 finite elements) was utilized and the calculations were stationary with a maximum of 25 iterations in each step.

obtained by the COMSOL Multiphysics software package (based on the same 3D nonlinear FE model used for the rod). Once again, the deflection under the infinitesimal strain assumption is included for comparison.

It is clear that the inextensional planar beam theory model agrees very well with the nonlinear FE solution based on the theory of elasticity. This is a significant result considering that the inextensional planar beam theory model is only a 1 DOF model. The conventional beam theory model on the other hand performs poorly and fails to even qualitatively capture the basic trend of the response. Here we note that in the conventional beam theory model there is a term that includes " $EA$ " (Eq. (21)). Yet, in the inextensional planar beam theory model any term including " $EA$ " drops out as a consequence of the derivations. Should we forcefully drop the term that features " $EA$ " in Eq. (21) we find that the response improves significantly although still does not match the accuracy of the inextensional planar motion model. For the wave propagation problem studied in Sections 5 and 6, omission of the term including " $EA$ " will also improve the performance of the conventional transverse motion model although in that case the response will not qualitatively follow the solution of the inextensional planar motion model (and therefore this omission will not be illustrated in the results we present in Section 6).

## 5. Wave dispersion under finite deformation

In this section we derive exact amplitude-dependent dispersion relations for harmonic wave propagation in a rod and in a flexural beam under finite deformation. We also obtain the explicit frequency versus wavenumber solutions - exactly for the rod problem and approximately for the flexural beam problem.

### 5.1. Rod: Exact analytical dispersion relation and solution

Using Eq. (2), we rewrite Eq. (12) as

$$\ddot{u} - c_0^2 u'' = \frac{1}{2} [3c_0^2 (u')^2 + c_0^2 (u')^3]', \quad (41)$$

where  $c_0 = \sqrt{E/\rho}$ . Equation (41) is integrable despite it being nonlinear. Differentiating (41) once with respect to  $s$  gives



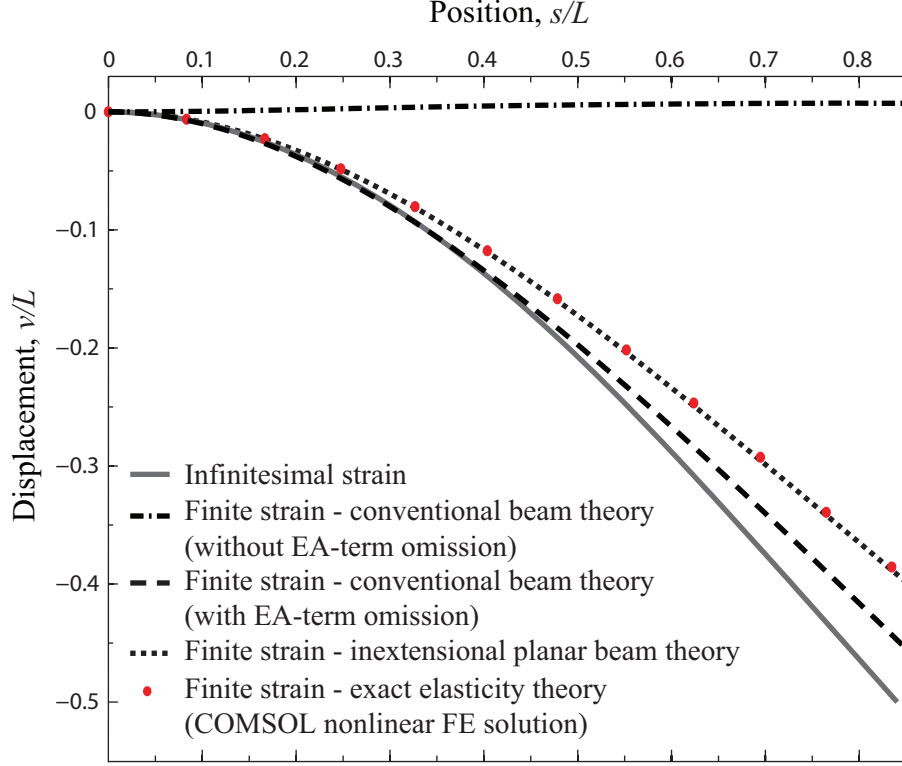


Figure 3: Static deflection of a clamped-free flexural beam ( $q_v L^3/8EJ = -0.5$ ).

$$(\ddot{u})' - c_0^2 u^{(3)} = \frac{1}{2} [3c_0^2 (u')^2 + c_0^2 (u')^3]'' . \quad (42)$$

Defining  $\bar{u} = u'$  and  $\tau = \omega t$ , where  $\omega$  is the frequency of a harmonic wave, Eq. (42) becomes

$$\omega^2 \bar{u}_{\tau\tau} - c_0^2 \bar{u}'' = \frac{1}{2} [3c_0^2 (\bar{u})^2 + c_0^2 (\bar{u})^3]'' . \quad (43)$$

Defining  $z = |\kappa|s + \tau$ , where  $\kappa$  is the wavenumber of a harmonic wave, we rewrite Eq. (43) as

$$\omega^2 \bar{u}_{zz} - c_0^2 \kappa^2 \bar{u}_{zz} = \frac{1}{2} \kappa^2 [3c_0^2 (\bar{u})^2 + c_0^2 (\bar{u})^3]_{zz} , \quad (44)$$

where now the explicit dependency on  $s$  and  $\tau$  has been eliminated. Integrating Eq. (44) twice leads to

$$\omega^2 \bar{u} - c_0^2 \kappa^2 \bar{u} = \frac{1}{2} \kappa^2 [3c_0^2 (\bar{u})^2 + c_0^2 (\bar{u})^3], \quad (45)$$

or,

$$(\omega^2 - c_0^2 \kappa^2) \bar{u} - \frac{c_0^2 \kappa^2}{2} (3\bar{u}^2 + \bar{u}^3) = 0. \quad (46)$$

We note that in our integration of Eq. (44) we get nonzero constants of integration in the form of polynomials in  $z$ . Since these represent secular terms we have set them all equal to zero in light of our interest in the dispersion relation. Selecting the positive root of Eq. (46) we get

$$\bar{u}(z) = \frac{-3 + \sqrt{1 + 8\omega^2/(c_0^2 \kappa^2)}}{2}. \quad (47)$$

Since  $\bar{u} = u_s$ , we recognize that  $\bar{u} = |\kappa|u_z$  and therefore Eq. (47) represents a first order nonlinear ordinary differential equation with  $z$  and  $u$  as the independent and dependent variables, respectively.

Now we return to Eq. (41) and consider for initial conditions a sinusoidal displacement field, with amplitude  $B$  and a zero phase in time, and a zero velocity field. Following the change of variables we have introduced, these initial conditions essentially correspond to the following restrictions on the  $\bar{u}(z)$  function given in Eq. (47):

$$\bar{u}(0) = |\kappa|B, \quad \bar{u}_z(0) = 0. \quad (48)$$

We note that since  $z$  describes a space-time wave phase, the restrictions given in Eq. (48) correspond to an initial wave phase and hence may be viewed as “initial conditions” on the wave phase. The importance of these initial conditions is that they incorporate the effect of the wave amplitude,  $B$ . Applying Eq. (48) to Eq. (47) allows us to use the latter to solve for  $\omega$  for a given value of  $\kappa$  at  $z = 0$ . Thus we obtain an exact dispersion relation for wave propagation in a rod under finite deformation, which is

$$\omega(\kappa; B) = \sqrt{\frac{2 + 3B|\kappa| + (B\kappa)^2}{2}} \omega_{\text{inf}}, \quad (49)$$

where  $\omega_{\text{inf}}$  is the frequency based on infinitesimal deformation,

$$\omega_{\text{inf}}(\kappa) = c_0|\kappa|. \quad (50)$$

By taking the limit,  $\lim_{B \rightarrow 0} \omega(\kappa; B)$ , in Eq. (49) we recover Eq. (50) which is the standard linear dispersion relation for a rod.

### 5.2. Conventional beam: Exact analytical dispersion relation

Differentiating Eq. (28) once with respect to  $s$  and omitting the external loads and gravity yields

$$-\rho A(\ddot{v})' + \rho J \left( \frac{\ddot{\alpha}}{r^2} \right)'' + (C_{vp})'' - (C_{vpp})''' = 0. \quad (51)$$

Defining  $\bar{v} = v'$ ,  $\tau = \omega t$  and  $z = \kappa s + \tau$ ,<sup>3</sup> we re-write Eq. (51) as

$$-\rho A \omega^2 (\bar{v}_{zz}) + \rho J \kappa^2 \omega^2 \left( \frac{\alpha_{zz}}{r^2} \right)_{zz} + \kappa^2 (C_{vp})_{zz} - \kappa^3 (C_{vpp})_{zzz} = 0. \quad (52)$$

Integrating Eq. (52) twice with respect to  $z$  gives us

$$-\rho A \omega^2 \bar{v} + \rho J \kappa^2 \omega^2 \frac{\alpha_{zz}}{r^2} + \kappa^2 C_{vp} - \kappa^3 (C_{vpp})_z = 0, \quad (53)$$

where  $\alpha = \tan^{-1} \bar{v}$  and

$$C_{vp} = 1/2 EA (\bar{v})^3 + EJ \kappa^2 \frac{(2 - 3r^2) \bar{v} (\bar{v}_z)^2}{2r^6} - EJ_f \kappa^4 \frac{\bar{v} (\bar{v}_z)^4}{r^{10}}, \quad (54a)$$

---

<sup>3</sup>From this point onwards, we replace  $|\kappa|$  with  $\kappa$  since only even-ordered functions of the wavenumber appear in the derived equations of motion.

$$C_{vpp} = EJ_f \kappa^3 \frac{(\bar{v}_z)^3}{2r^8} - EJ\kappa \frac{(1 - 3r^2)\bar{v}_z}{2r^4}, \quad (54b)$$

$$r = \sqrt{1 + (\bar{v})^2}. \quad (54c)$$

In deriving Eq. (53) we set the constants of integration to zero and thus drop out the secular terms as we did for the rod model. Furthermore, we recognize that  $\bar{v} = v_s$  and therefore  $\bar{v} = |\kappa|v_z$ . In an analogous manner to the rod problem (see Sec. 5.1), we write the following initial conditions for the wave phase:

$$\bar{v}(0) = B\kappa, \quad \bar{v}_z(0) = 0. \quad (55)$$

Eq. (53), which is a function of  $B$ , can be solved numerically using a standard root finding technique to obtain the explicit dispersion relationship between frequency and wavenumber for a conventional beam under finite deformation.

### 5.3. Inextensional planar beam: Exact analytical dispersion relation

Differentiating Eq. (38) once with respect to  $s$  and omitting the external loads and gravity yields

$$-\rho A(\ddot{v})' + \rho J \left( \frac{\ddot{\alpha}}{r^2} \right)'' + (C_{vp})'' - (C_{vpp})''' = 0. \quad (56)$$

Defining  $\bar{v} = v'$ ,  $\tau = \omega t$  and  $z = \kappa s + \tau$ , Eq. (56) is re-written as

$$-\rho A \omega^2 (\bar{v}_{zz}) + \rho J \kappa^2 \omega^2 \left( \frac{\alpha_{zz}}{r^2} \right)_{zz} + \kappa^2 (C_{vp})_{zz} - \kappa^3 (C_{vpp})_{zzz} = 0. \quad (57)$$

Integrating Eq. (57) twice leads to

$$-\rho A \omega^2 \bar{v} + \rho J \kappa^2 \omega^2 \frac{\alpha_{zz}}{r^2} + \kappa^2 C_{vp} - \kappa^3 (C_{vpp})_z = 0, \quad (58)$$

where  $\alpha = \tan^{-1} \bar{v}$  and

$$C_{vp} = - \left( J + \frac{\kappa^2 J_f (1 + 2\bar{v}^2) \bar{v}_z^2}{2(1 - \bar{v}^2)} \right) \frac{E \kappa^2 \bar{v} \bar{v}_z^2}{(1 - \bar{v}^2)^2} - \left( J + \frac{3\bar{v}_z^2}{2(1 - \bar{v}^2)} \right) \frac{E \kappa^2 \bar{v}^2 \bar{v}_{zz}}{1 - \bar{v}^2}, \quad (59a)$$

$$C_{vpp} = \left( J + \frac{J_f \kappa^2 \bar{v}_z^2}{2(1 - \bar{v}^2)} \right) E \kappa \bar{v}_z. \quad (59b)$$

In deriving Eq. (58) we set the constants of integration to zero in order to drop out the secular terms as we did for the rod and conventional beam models. Furthermore, and as we stated for the conventional beam model,  $\bar{v} = v_s$  and therefore  $\bar{v} = |\kappa|v_z$ . Following the same approach as in Sections 5.1 and 5.2, we use the initial conditions stated in Eq. (55) for the wave phase. Subsequently, Eq. (58), which is a function of  $B$ , can be solved numerically using a standard root finding technique to obtain the explicit dispersion relationship between frequency and wavenumber for an inextensional planar beam under finite deformation.

## 6. Results and discussion

### 6.1. Finite-deformation dispersion curves

Two amplitude-dependent finite-deformation dispersion curves for an infinite rod based on Eq. (49) are plotted in Fig. 4. These dispersion curves provide an exact fundamental description of how an elastic harmonic wave locally, and instantaneously, disperses in an infinite rod under the dynamic condition of amplitude-dependent finite deformation. Superimposed in the same figure is the dispersion curve based on infinitesimal deformation, i.e., Eq. (50). We observe that the deviation between a finite-deformation curve and the infinitesimal-deformation curve increases gradually with wavenumber, and the effect of the wave amplitude on this deviation appears to be relatively steady - in the wavenumber range considered - as  $B$  is increased. More thorough inspection of this deviation is provided in Section 6.2.

In addition, the results from standard FE simulations of a finite version of the rod with length  $L$  are presented. A prescribed sinusoidal displacement with frequency  $\hat{\omega}$  and amplitude  $\hat{B}$ , i.e.  $u(L, t) = \hat{B} \sin \hat{\omega} t$ , was applied to the tip of the rod with free-free boundary conditions. The finite-deformation FE model consisted of 60 piecewise linear elements with equal lengths, and each node consisted of two degrees of freedom,  $u$  and  $u'$ . Equal time steps of  $10^{-4}$  [s] were considered in the numerical integration which was implemented using MATLAB's *ode113* solver [41]. The wavenumber has been recorded by observing the wavelength after one period of temporal oscillation of the tip (i.e., excitation point) of the rod, and plotted as a function of frequency  $\hat{\omega}$  for two given amplitudes. This recording was possible because at the vicinity of

the excitation point the wave's harmonic form was effectively still maintained during the first oscillation cycle. The data points from this simulation (of a finite rod) match very well with the analytically derived exact dispersion curve (corresponding to an infinite rod). While the wave considered at the tip of the excited rod will evolve, under finite strain, into a complex form as it propagates into the rod, this correlation provides a validation that a given harmonic wave will locally and instantaneously disperse in a manner exactly as described by Eq. (49). A second set of independent simulation data is also shown in the figure. This set corresponds to the response due to initial sinusoidal displacements at a prescribed wavenumber (applied at a state when the rod is at rest). Here we measured the frequency of oscillation as the wave propagates considering the first temporal cycle. The simulation parameters are the same to those used in the runs where an initial end-point displacement is prescribed. As illustrated in the figure, this simulation provides yet another validation of the analytical dispersion relation given by Eq. (49).

In Fig. 5, we present dispersion curves for the conventional and inextensional planar beam models. For each of the models, we show results for two different amplitudes,  $B$ . In the interest of generality, the amplitude is considered in relation to the beam's cross-sectional radius,  $a$ . The explicit relationship between frequency and wavenumber is obtained by numerically solving for the roots of Eq. (53) for the conventional beam model and the roots of Eq. (58) for the inextensional planar beam model. Also shown in Fig. 5 is the dispersion curve based on infinitesimal deformation, which is

$$\omega_{\text{inf}}(\kappa) = \frac{c_0 r_0 \kappa^2}{\sqrt{1 + r_0^2 \kappa^2}}. \quad (60)$$

The finite-strain curve of the conventional beam model shows a rapid change in slope at low frequencies compared to the infinitesimal-strain curve, which suggests poor performance as was seen in the static case. The inextensional beam response on the other hand shows asymptotic convergence with the linear dispersion as  $\omega \rightarrow 0$  and the deviation grows slowly with  $\kappa$ . We can also observe the effect of the wave amplitude on the dispersion: as  $B$  increases the dispersion curve rises at an increasing rate. Further comparison between the finite-deformation and infinitesimal-deformation responses is provided in Section 6.2.

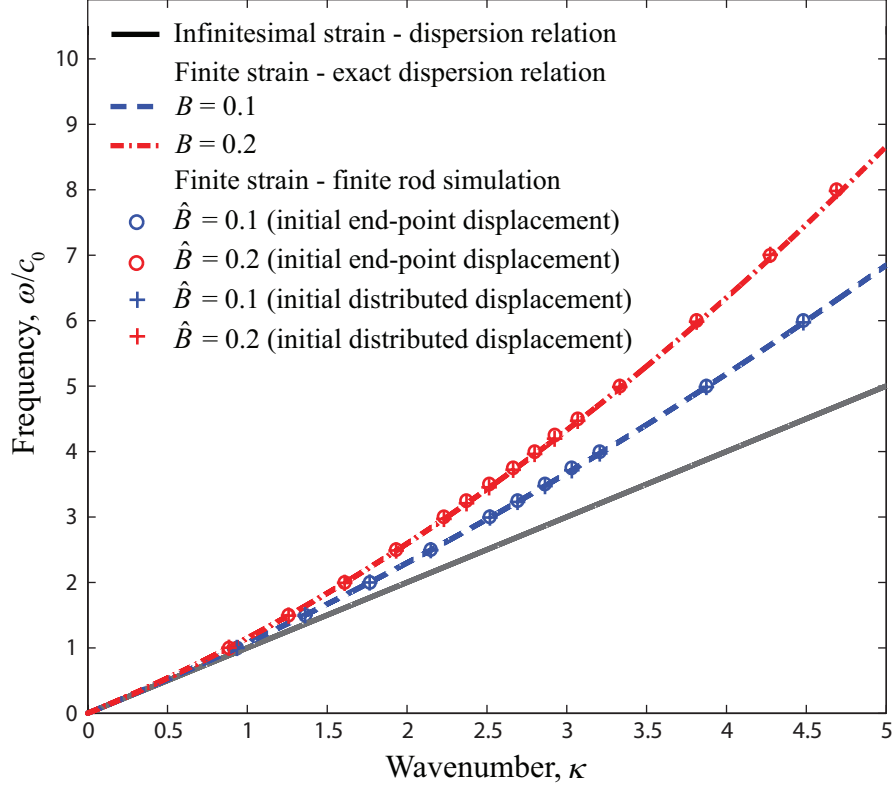


Figure 4: Frequency dispersion curves for a rod. The finite-strain dispersion relation is based on Eq. (49); the infinitesimal strain dispersion relation is based on Eq. (50).

Figure 6 shows the group velocity versus wavenumber curves for the same cases considered in Figs. 4 and 5. The group velocity is defined as  $c_g = \partial\omega/\partial\kappa$ . The figure puts on view the significant qualitative transformation that emerges when finite deformation is incorporated in wave propagation analysis. For axial waves the group velocity, which is otherwise constant, is now varying with  $\kappa$ . And for flexural waves the group velocity follows a nonlinear function with  $\kappa$  in contrast to the linear trend for the infinitesimal-deformation model. Needless to say, the intensity of these finite-deformation effects on the group velocity increases with  $B$  as mentioned in our discussion of the frequency dispersion curves. A phase velocity dispersion diagram may also be generated, and from Figs. 4 and 5 it is clear that the trends will be similar to Fig. 6.

The dispersion characteristics presented provide an elucidation of the non-

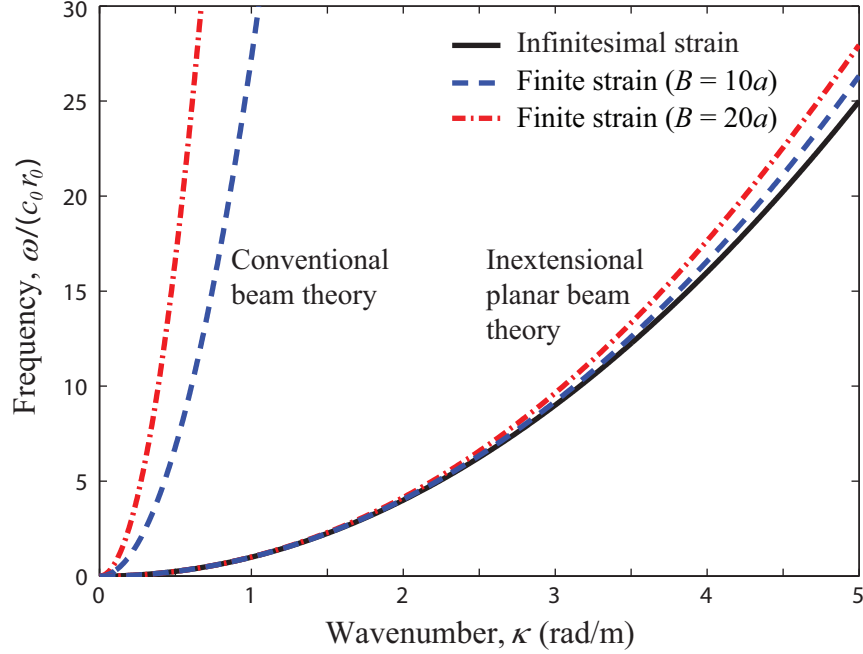


Figure 5: Frequency dispersion curves for a conventional beam and an inextensional planar beam. The finite-strain curves represent exact solutions of Eqs. (53) and (58), respectively, evaluated by numerical root-finding. The infinitesimal-strain curve (based on Eq. (60)) is also shown.

linear, finite-deformation dynamics of rods and beams particularly for long structures or when the focus is on high frequency/short wavelength behavior where a standard analysis based on superposition of standing waves is generally not effective [42]. From a conceptual point of view, an increase in group velocities as seen in Fig. 6 is particularly significant in the study of waves where the rate and intensity of energy propagation is consequential, such as in seismic waves [13, 14]. It is also relevant to the study of the speed of propagation of dislocations and cracks considering that large amplitudes have been observed near slip planes and crack tips [11, 12] (recalling that the phase and group velocities change with deformation amplitude). Future work will introduce appropriate extensions in the implementation of our methodology to address the specific geometric and material characteristics of these applications.

From an engineering design perspective, the amplitude-dependent dispersion behavior we observe in Figs. 4, 5 and 6 potentially could be of benefit



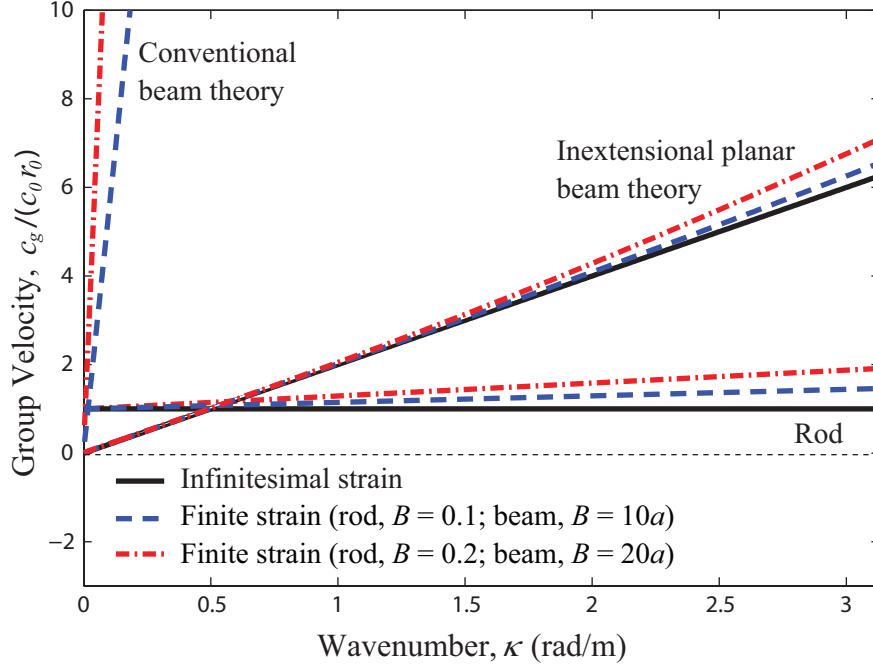


Figure 6: Group velocity dispersion curves for a rod, a conventional beam and an inextensional planar beam under finite strain.

to numerous applications; for example, the frequency shifts observed suggest possible utilization of regular rods and beams as amplitude-dependent wave propagation filters. Further utilization is possible when these properties are considered in conjunction with other avenues for design such as the introduction of periodicity [43–45]. Here we note that the derived finite-strain dispersion relations can be incorporated directly into transfer matrix models of 1D periodic media, which will be the focus of future research.

### 6.2. Comparison with infinitesimal-deformation dispersion curves

Figure 7 presents the percentage deviation in the dispersion curves when finite deformation is incorporated compared to when infinitesimal deformation is assumed (evaluated at  $\kappa = \pi$ ). Clearly the higher the wave amplitude, the higher the deviation. For a rod, the deviation follows a concave curve (increases at a decreasing rate); whereas for an inextensional planar beam it follows a convex curve (increases at an increasing rate). The level of deviation for a given wave amplitude is considerably higher for longitudinal waves in a rod compared to transverse waves in the inextensional planar beam.

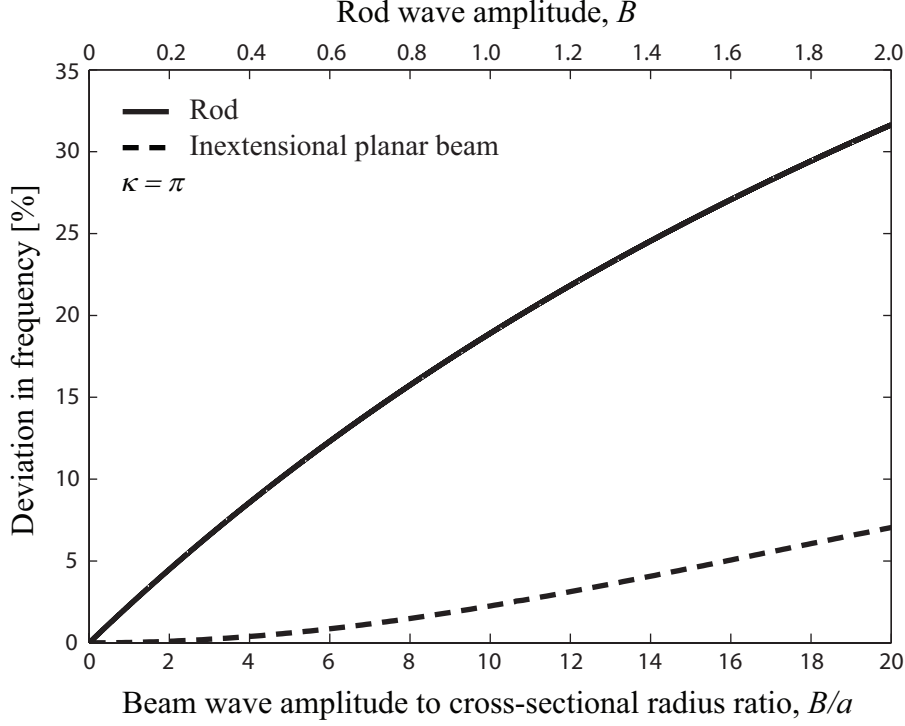


Figure 7: Percentage deviation in frequency when the dispersion curves are based on infinitesimal strain versus finite strain (evaluated at  $\kappa = \pi$ ).

### 6.3. Effect of the 4<sup>th</sup> moment of area, $J_f$

In this section we examine the effect of the 4<sup>th</sup> moment of cross-sectional area,  $J_f$ , on the finite-deformation dispersion relations for flexural beams. If, by way of example, we consider a beam with a circular cross section of radius  $a$ , then the terms  $r_0$  and  $r_f$  would each be a function of  $a$ , i.e.,  $r_0 = \sqrt{J/A} = a/2$  and  $r_f = \sqrt{J_f/A} = a^2/2\sqrt{2}$ . Hence we get  $r_f/r_0 = a/\sqrt{2}$  from which we can deduce that any term that contains  $J_f$  diminishes when the cross-sectional area is small. Fig. 8 shows the effect of omission of all terms that contain  $J_f$  in both the conventional and inextensional planar beam models. From the figure we note that for a ratio of cross-sectional radius to wave amplitude,  $a/B$ , smaller than approximately 0.025, the effect of omitting the terms that contain  $J_f$  in Eqs. (29) and (39) is negligible. However, for higher values of this ratio, the error introduced by this omission increases dramatically.

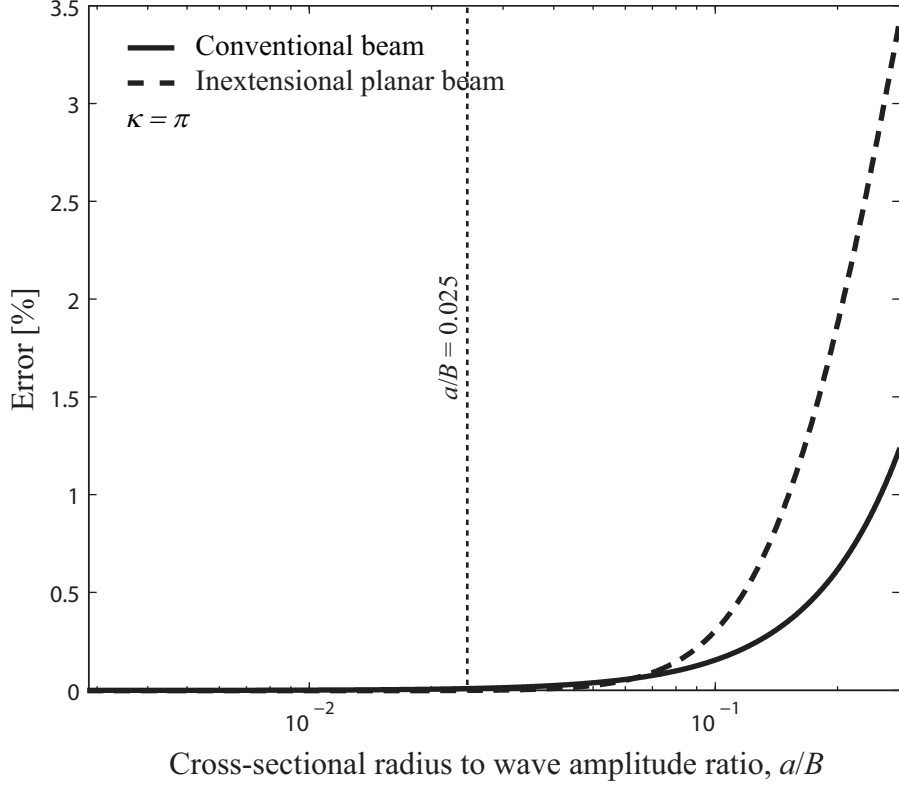


Figure 8: Percentage error in frequency due to omission of terms including  $J_f$  in Eqs. (28) and (39) for conventional and inextensional planar beams (evaluated at  $\kappa = \pi$ ).

## 7. Conclusions

We have derived and solved an exact dispersion relation for finite-strain wave propagation in a slender rod and an Euler-Bernoulli beam. This represents the first derivation of dispersion relations for elastic media under finite deformation, providing an analogy to the derivation of anharmonic (nonlinear) dispersion relations of crystals in condensed matter physics.

For axial motion (i.e., the rod problem), the closed-form exact frequency versus wavenumber solution was derived as a function of wave amplitude. The solution matched very well with data points obtained from high-resolution FE simulations of a finite rod under finite deformation. For transverse motion (i.e., the conventional and inextensional planar beam problems), an approximate solution was obtained by numerically solving for the roots of the derived exact dispersion relation. A key aspect of the derivations that lead to the

dispersion relation for each of these problems involves the introduction of a space-time wave phase,  $z$ , and the development of a relationship for which the solution at  $z = 0$  gives the amplitude-dependent dispersion relation.

The results show that finite deformation causes the frequency (and therefore the phase and group velocity) dispersion curves to shift for both axial and flexural waves in comparison to when infinitesimal deformation is assumed. The level at which these nonlinear effects take place is dependent on the amplitude of the travelling wave, and the degree of shift in the dispersion curves increases with wavenumber. Both the rod and inextensional beam solutions display asymptotic convergence to the corresponding linear, infinitesimal-strain solution at low frequencies and at low wave amplitudes. For our choice of Cauchy stress and Green-Lagrange strain, all observed shifts are positive, i.e., the curves rise with finite deformation. Future work will examine the response based on other stress and strain measures, which in itself will serve as a rigorous characterization of the spectral properties of these measures. The results also show, for wave dispersion as well as static deflection, that a coupling between the axial and transverse motions is necessary for an accurate description of the response.

Our analysis provide a means for elucidating the nonlinear dynamics of rods and flexural beams particularly for long structures or when the focus is on high frequency/short wavelength behavior. It also has implications on the study of wave phenomena in a broader range of problems where large elastic motion takes place. Examples where large deformations have been experimentally observed include waves produced by cracks and dislocations (problems of great importance in seismology, fracture mechanics and plasticity). In these problems, the standard dispersion relations based on infinitesimal motion cannot predict any alterations in the speed of sound due to the intensity of the motion, as we observed in Fig. 6 for the 1D models considered. While our present formulations consider linear constitutive relations (in order to isolate the effect of finite motion), the proposed methodology is applicable to problems that also exhibit material nonlinearity - which would be necessary for the applications mentioned above. From an engineering design perspective, the amplitude-dependent shifts in frequency, phase and group velocity in the dispersion spectrum provide promising avenues for the development of novel materials, structures and devices.

The presented analytical formalism for dispersion analysis under finite deformation lays the foundation for systematic extensions to more complex 1D models (e.g., rods/beams incorporating lateral inertia in longitudinal mo-

tion, beams incorporating corotational motion, higher DOF beams) as well as multi-dimensional models (e.g., thin plates and shells, 2D plain stress/strain models, semi-infinite surfaces, 3D rods and plates, bulk media).

## References

- [1] S. D. Poisson, Mémoire sur l'équilibre et le mouvement des corps élastique (Memorandum on equilibriums and the movement of elastic bodies), Mémoires de l'Académie des Sciences de l'Institut de France 8 (1829) 357–570. (Read to the Paris Academy on 14 April 1828).
- [2] A. L. Cauchy, Exercices de Mathématiques (Mathematics Exercises), Paris (1830).
- [3] K. F. Graff, Wave motion in elastic solids, Dover Publications, New York, 1991.
- [4] A. Ben-Menahem, A concise history of mainstream seismology: Origins, legacy, and perspectives, Bulletin of the Seismological Society of America 85 (1995) 1202–1225.
- [5] R. N. Thurston, Waves in solids, in: C. Truesdell (Ed.), Mechanics of Solids, volume 4, Springer-Verlag, Berlin, 1984, pp. 109–308.
- [6] J. D. Achenbach, Wave propagation in elastic solids, North-Holland, Amsterdam, 1987.
- [7] A. H. Nayfeh, D. T. Mook, Nonlinear Oscillations, Wiley-VCH, New York, 1995.
- [8] M. Destrade, G. Saccomandi, Introduction to the special issue on waves in non-linear solid mechanics, International Journal of Non-linear Mechanics 44 (2009) 445–449.
- [9] S. W. Shaw, C. Pierre, Normal modes for nonlinear vibratory systems, Journal of Sound and Vibration 164 (1993) 85–124.
- [10] G. Kerschen, K. Worden, A. F. Vakakis, J.-C. Golinval, Past, present and future of nonlinear system identification in structural dynamics, Mechanical Systems and Signal Processing 20 (2006) 505–592.

- [11] P. Gumbsch, H. Gao, Dislocations faster than the speed of sound, *Science* 283 (1999) 965–968.
- [12] A. J. Rosakis, O. Samudrala, D. Coker, Cracks faster than the shear wave speed, *Science* 284 (1999) 1337–1340.
- [13] M. K. Sen, P. L. Stoffa, Nonlinear one-dimensional seismic waveform inversion using simulated annealing, *Rivista Del Nuovo Cimento* 56 (1991) 1624–1638.
- [14] L. A. Ostrovsky, P. A. Johnson, Dynamic nonlinear elasticity in geomaterials, *Rivista Del Nuovo Cimento* 24 (2001) 1–46.
- [15] Y. Zheng, R. G. Maev, I. Y. Solodov, Nonlinear acoustic applications for material characterization: A review, *Canadian Journal of Physics* 77 (1999) 927–967.
- [16] K. E.-A. Van Den Abeele, P. A. Johnson, A. Sutin, Nonlinear elastic wave spectroscopy (NEWS) techniques to discern material damage, part I: Nonlinear wave modulation spectroscopy, *Research in Nondestructive Evaluation* 12 (2000) 17–30.
- [17] B. Ward, A. C. Baker, V. F. Humphrey, Nonlinear propagation applied to the improvement of resolution in diagnostic medical ultrasound, *Journal of the Acoustical Society of America* 101 (1997) 143–154.
- [18] C. Truesdell, General and exact theory of waves in finite elastic strain, *Archive for Rational Mechanics and Analysis* 8 (1961) 263–296.
- [19] A. E. Green, A note on wave propagation in initially deformed bodies, *Journal of the Mechanics and Physics of Solids* 11 (1963) 119–126.
- [20] R. W. Ogden, *Non-linear elastic deformations*, Dover Publications, New York, 1997.
- [21] P. Boulanger, M. Hayes, Finite-amplitude waves in deformed mooney-rivlin materials, *Quarterly Journal of Mechanics and Applied Mathematics* 45 (1992) 575–593.
- [22] P. Boulanger, M. Hayes, C. Trimarco, Finite-amplitude plane waves in deformed Hadamard elastic materials, *Geophysical Journal International* 118 (1994) 447–458.

- [23] M. Destrade, G. Saccomandi, Nonlinear transverse waves in deformed dispersive solids, *Wave Motion* 45 (2008) 325–336.
- [24] A. N. Norris, Finite amplitude waves in solids, In: M. F. Hamilton and D. T. Blackstock (Eds.), *Nonlinear Acoustics*, 263–277, Academic Press, San Diego (1999).
- [25] B. Auld, *Acoustic fields and waves in solids*, Krieger, Malabar, Florida, 1990.
- [26] W. J. N. de Lima, M. F. Hamilton, Finite-amplitude waves in isotropic elastic plates, *Journal of Sound and Vibration* 265 (2003) 819–839.
- [27] M. Deng, Analysis of second-harmonic generation of lamb modes using a modal analysis approach, *Journal of Applied Physics* 94 (2003) 4152–4159.
- [28] S. S. A. Srivastava, I. Bartoli, F. L. di Scalea, Higher harmonic generation in nonlinear waveguides of arbitrary cross-section, *Journal of the Acoustical Society of America* 127 (2010) 2790–2796.
- [29] T. Wright, Nonlinear-waves in rods: results for incompressible elastic-materials, *Studies in Applied Mathematics* 72 (1985) 149–160.
- [30] B. D. Coleman, D. C. Newman, On waves in slender elastic rods, *Archive for Rational Mechanics and Analysis* 109 (1990) 39–61.
- [31] A. M. Samsonov, Nonlinear strain waves in elastic waveguides, In: A. Jeffrey, J. Engelbregt (Eds.), *Nonlinear Waves in Solids*, 349–382, Springer, New York (1994).
- [32] H.-H. Dai, Model equations for nonlinear dispersive waves in a compressible Mooney-Rivlin rod, *Acta Mechanica* 127 (1998) 193–207.
- [33] H.-H. Dai, Y. Huo, Solitary shock waves and other travelling waves in a general compressible hyperelastic rod, *Proceedings of the Royal Society of London Series A - Mathematical, Physical and Engineering Sciences* 456 (2000) 331–363.
- [34] S.-Y. Zhang, Z.-F. Liu, Three kinds of nonlinear dispersive waves in elastic rods with finite deformation, *Applied Mathematics and Mechanics (English Edition)* 29 (2008) 909–917.

- [35] M. H. Abedinnasab, M. I. Hussein, Analysis of elastic wave propagation in nonlinear beams, ASME Conference Proceedings Volume 1: 23rd Biennial Conference on Mechanical Vibration and Noise, Parts A and B, Paper no. DETC2011-48672 (2011) 207–212.
- [36] M. R. M. C. da Silva, C. C. Glynn, Non-linear flexural-flexural-torsional dynamics of inextensional beams, I: equations of motion, Journal of Structural Mechanics 44 (1978) 437–443.
- [37] A. H. Nayfeh, P. F. Pai, Linear and Nonlinear Structural Mechanics, John Wiley and Sons, Hoboken, New Jersey, 2004.
- [38] W. Lacarbonara, H. Yabuno, Refined models of elastic beams undergoing large in-plane motions: Theory and experiment, Int. J. Solids Struct. 43 (2006) 5066–5084.
- [39] M. H. Abedinnasab, H. Zohoor, Y.-J. Yoon, Exact formulations of non-linear planar and spatial Euler-Bernoulli beams with finite strains, Proceedings of the Institution of Mechanical Engineers, Part C: Journal of Mechanical Engineering Science 226 (2012) 1225–1236.
- [40] Comsol Inc., 2010. URL: <http://www.comsol.com>.
- [41] The MathWorks Inc., 2009. URL: <http://www.mathworks.com>.
- [42] M. Behbahani-Nejad, N. C. Perkins, Freely propagating waves in elastic cables, Journal of Sound and Vibration 196 (1996) 189–202.
- [43] M. I. Hussein, G. M. Hulbert, R. A. Scott, Dispersive elastodynamics of 1d banded materials and structures: analysis, Journal of Sound and Vibration 289 (2006) 779–806.
- [44] M. I. Hussein, G. M. Hulbert, R. A. Scott, Dispersive elastodynamics of 1d banded materials and structures: design, Journal of Sound and Vibration 307 (2007) 865–893.
- [45] L. Liu, M. I. Hussein, Wave motion in periodic flexural beams and characterization of the transition between Bragg scattering and local resonance, Journal of Applied Mechanics 79 (2012) 011003.